Dual-Band SIW Filter With Widely Separated Passbands Based on TE_{101} and TE_{301} Modes

Yilong Zhu[#*1], Yuandan Dong[#2], Xun Luo[#3], Jens Bornemann[*4]
[#]University of Electronic Science and Technology of China, Chengdu, Sichuan, China
[*]Department of Electrical and Computer Engineering, University of Victoria, Victoria, BC, Canada
[1]yilong@std.uestc.edu.cn, [2]ydong@uestc.edu.cn, {[3]xun-luo, [4]j.bornemann}@ieee.org

***Abstract*—In this paper, a novel dual-band substrate integrated waveguide (SIW) filter with widely separated passbands is presented, which is realized by dual-mode TE_{101} and TE_{301} resonances. To make the TE_{301} mode create the second passband, two novel techniques to suppress the TE_{201} mode are proposed and discussed. The proposed techniques excite the TE_{201} mode but either block its coupling path or cancel its effect at the output port, which can be identified as mode blocking and mode cancelling, respectively. They show a merit of introducing an extra transmission zero, which is beneficial to enhance the out-of-band rejection. To verify the concept, a dual-band filter prototype operating at 6.5 and 11 GHz is designed and fabricated, which shows a good electrical performance and a compact size.**

***Keywords*—Compact size, dual-band filter, mode blocking, mode cancelling, widely separated passbands.**

I. Introduction

To meet challenges of future generations of satellite systems integrating transmit (TX) and receive (RX) RF front ends into a compact subsystem, dual-band microwave components, and especially filters with widely separated passbands, have been demonstrated, whose two passbands can be used as TX and RX frequency bands [1], [2].

For compactness and integration of communication systems, planar fabrication processes, such as microstrip and substrate integrated waveguide (SIW) technologies, have been widely used to implement dual-band filters with widely separated passbands. Generally, microstrip dual-band filters show higher passband frequency ratios with compact size, but their unloaded quality factors (Q_u) are too low to be operated at high frequencies [3-9]. In contrast, SIW technology can be used to design high-frequency, even mm-wave filters due to larger Q_u and power handling capability. For example, dual-band filters based on TE_{101} and TE_{201} (or TE_{102}) modes are reported in [10-13], but the passband frequency ratios are limited within 1.5. Although the frequency ratio can be expanded with capacitive load in [14], it is unavoidable to use multilayer structures. By using half-mode SIW (HMSIW) technology [15], the frequency ratio of the dual-band filters can be extended to 1.7, but they would suffer from increased insertion loss (IL) due to radiation effects from the open edges of HMSIW cavities.

In this paper, a dual-band SIW filter based on TE_{101} and TE_{301} modes is proposed. To make the TE_{301} mode create the second passband, suppression of the TE_{201} mode is required. Two novel suppression techniques, which are named mode blocking and mode cancelling, are proposed, analyzed and applied in this paper. Different from the conventional technique to disable the excitation of the TE_{201} mode, the proposed techniques excite the TE_{201} mode but either block its coupling path or cancel its effect at the output port, which exhibit an advantage of creating an extra transmission zero (TZ). Experimental verification is demonstrated by a 3rd-order dual-band filter operating at 6.5 and 11 GHz, which presents widely separated passbands with a frequency ratio of 1.69.

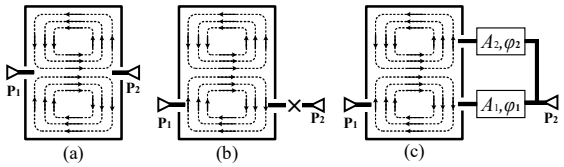

Fig. 1. (a) Typical technique to suppress the TE_{201} mode by placing feeding ports at the centre of the SIW cavity. (b) First proposed suppression method by preventing the propagation of the TE_{201} mode. (c) Second proposed method to suppress the TE_{201} mode by using mode cancelling at the output port.

II. Novel Techniques To Suppress TE_{201} Mode

A. Conventional Technique to Suppress TE_{201} Mode

As shown in Fig. 1(a), the typical method to suppress the TE_{201} mode is to place feeding ports at the center of the SIW cavity, which disables the TE_{201} mode excitation and most effectively excites the TE_{101} and TE_{301} modes.

B. Novel Techniques: Mode Blocking and Mode Cancelling

Instead of disabling the resonance of the TE_{201} mode, the proposed techniques excite the TE_{201} mode but block its coupling paths or cancel its effect at the output.

Fig. 1(b) shows the diagram of the proposed technique. The TE_{201} mode is excited by the asymmetric input port, but it could be neglected if we can block its coupling path to the output. To achieve mode blocking, a feasible way is proposed by inserting a microstrip resonator between two SIW cavities. If the resonant frequency of the microstrip resonator is similar to that of the TE_{201} mode, a coupling path between the resonators would be created, otherwise the TE_{201} mode would be blocked. The detailed discussion is presented in Section III.

Fig. 1(c) shows the second technique to suppress the TE_{201} mode, which is called mode cancelling. In this diagram, two coupling paths for the TE_{201} mode are created from the SIW cavity to the output port. Considering such a scenario, if the signals of the two coupling paths have the same strength (A_1=A_2) but a phase difference of 180° (φ_1-φ_2=180°), the TE_{201} mode components would cancel each other out (mode cancelling) when they arrive at the output port.

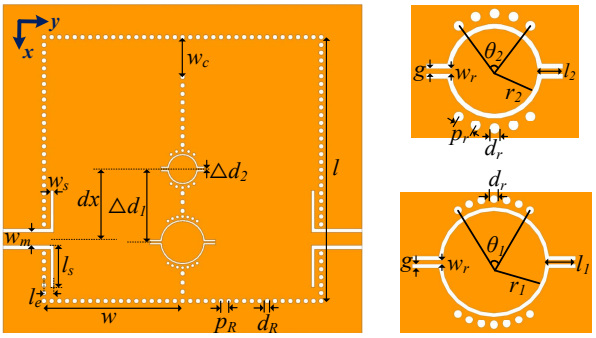

Fig. 2. Layout of the proposed dual-band SIW filter based on TE_{101} and TE_{301} modes and magnified circular patch resonators. Initial dimensions in mm: l = 32.5, l_s = 5.2, l_e = 1.2, w = 17, w_s = 0.4, w_m = 1.57, g =0.2, w_c = 4.9, dx = 8.6, $\triangle d_1$ = 9, $\triangle d_2$ = 0, d_R = 0.6, p_R < 1, d_r = 0.4, p_r < 0.8, w_r = 0.2, θ_1 = 69°, r_1 = 2.551, l_1 = 1.5, θ_2 = 76°, r_2 = 1.684, l_2 = 1.

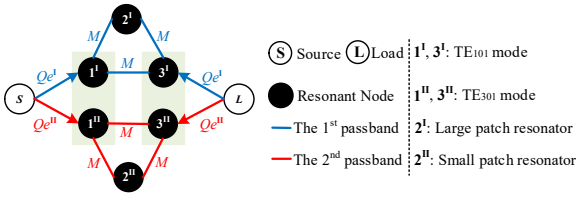

Fig. 3. Coupling schematic topology of the proposed dual-band SIW filter based on TE_{101} and TE_{301} modes.

III. Dual-Band SIW Filter Design And Analysis

A. Filter Design and Analysis

Fig. 2 shows the configuration of the proposed dual-band filter, which is based on dual-mode resonances of SIW TE_{101} and TE_{301} modes. The TE_{101} mode is used to generate the first passband, while the TE_{301} mode creates the second one. Two microstrip circular patch resonators etched between the SIW cavities, which resonate at the same frequencies as the TE_{101} and TE_{301} modes, respectively, are utilized to couple to these two SIW modes. The fan-shape via-arrays, which are placed around the patch resonators, are used to adjust the coupling strength between the SIW and patch resonators.

In this filter configuration, the TE_{201} mode is suppressed due to lacking a suitable patch resonator to couple into, thus leading to the mode excited but restricted in the first SIW cavity. However, since the large patch resonator is located at the position where the TE_{201} mode shows the maximum field distributions, the mode can still be partially coupled between the resonators. To further suppress it, an inductive coupling window with a width of w_c is constructed between the SIW cavities, which can be viewed as the second coupling path to cancel out the signal leaked through the large patch resonator. Additionally, the inductive window also introduces a cross coupling between the two SIW cavities.

In terms of such a filter configuration, the coupling schematic topology of the proposed dual-band filter is depicted in Fig.3, where the superscripts I and II denote the first and second passband. R1 and R3 represent TE_{101} and TE_{301} modes, respectively, and R2 denotes the patch resonators. Note that the coupling between any two resonators is magnetic.

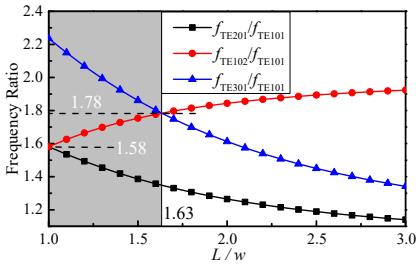

Fig. 4. Frequency ratio analysis of the proposed dual-band filter.

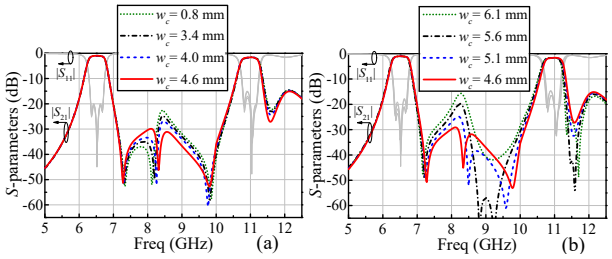

Fig. 5. (a) Simulated *S*-parameters versus coupling window width w_c increasing from 0.8 to 4.6 mm. (b) Simulated *S*-parameters versus coupling window width w_c increasing from 4.6 to 6.1 mm.

B. Achievable Frequency Ratio and Coupling Matrix

To explore the achievable frequency ratio by using TE_{101} and TE_{301} modes, four resonance modes, including TE_{101}, TE_{201}, TE_{102}, and TE_{301} modes, are analyzed. The frequency ratio of these higher-order modes to TE_{101} one can be deduced as

$$\frac{f_{TE201}}{f_{TE101}}=\sqrt{1+\frac{3}{1+(L/w)^2}},\quad \frac{f_{TE102}}{f_{TE101}}=\sqrt{1+\frac{3(L/w)^2}{1+(L/w)^2}},\quad \frac{f_{TE301}}{f_{TE101}}=\sqrt{1+\frac{8}{1+(L/w)^2}}$$

where L and w are equivalent length and width of the SIW cavities. Fig. 4 plots the theoretical frequency-ratio curves versus the aspect ratio L/w. As is seen, to use the TE_{301} mode the second higher-order mode, an aspect ratio L/w >1.63 is required, leading to an achievable frequency ratio of 1.78.

To validate the proposed filter, a prototype with 20-dB return loss for each passband is synthesized. The center frequencies are set at f_1 =6.5 GHz and f_2 =11 GHz (f_2/f_1=1.69), with qual-ripple bandwidths of 360 MHz (Δ_1=5.5%) and 380 MHz (Δ_2=3.5%), respectively. A TZ is placed at the right side of each passband. The coupling matrix and external quality factors can be obtained by the synthesis procedure in [16] as

$$Q_e^I=16.5,\qquad Q_e^{II}=25.4,$$

$$M^I=\begin{bmatrix}0.004 & 0.053 & 0.014\\ 0.053 & -0.013 & 0.053\\ 0.014 & 0.053 & 0.004\end{bmatrix},\ M^{II}=\begin{bmatrix}0.004 & 0.033 & 0.012\\ 0.033 & -0.012 & 0.033\\ 0.012 & 0.033 & 0.004\end{bmatrix}$$

C. Suppression of TE_{201} Mode

Two techniques, which are called mode blocking and mode cancelling, are utilized to suppress the TE_{201} mode. Due to the lack of a suitable patch resonator between the two SIW cavities, the TE_{201} mode would be blocked in the first cavity. However, the signals can be still partially coupled through the large patch resonator. As shown in Fig. 5(a), when the inductive window is closed (namely w_c = 0.8mm), the out-of-band rejection level is approximately 20 dB due to the leakage of the TE_{201} mode

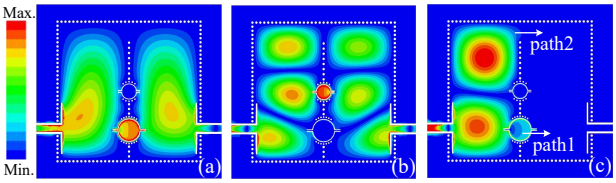

Fig. 6. Electric field distributions of the proposed filter at (a) 6.5 GHz, (b)11 GHz, and (c) 8.3 GHz.

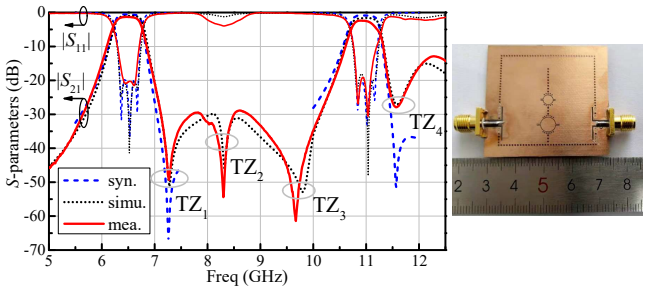

Fig. 7. Photograph of the fabricated dual-band filter, and its synthesized, simulated and measured *S*-parameters.

through the large patch resonator. By increasing the width of the inductive window, namely increasing the signal strength through this coupling path, the rejection level can be enhanced to 30 dB with a TZ created when w_c = 4.6 mm. As presented in Fig. 5(b), a further increase of the inductive window width would reduce the rejection level because the TE_{201} mode is increasingly coupled to the output port through the inductive window. Therefore, mode cancelling can only occur when the signals transferred by the large patch resonator and the inductive window have equal strength.

Fig. 6 shows the electric field distributions of the two passbands and the rejection band at 8.3 GHz. As shown, the TE_{101} and TE_{301} modes are coupled between the SIW cavities through the large and small patch resonators, respectively, while the TE_{201} mode is restricted to the first cavity. Although a small part of the signal leaks through the large patch resonator, the TE_{201} mode can be further suppressed by the dual-path mode cancelling shown in Fig 6(c).

IV. Fabrication, Measurement, And Discussion

To demonstrate the proposed design concept, a filter prototype fabricated on Rogers RT/Duriod 5880 substrate is measured for validation. Fig. 7 shows synthesized, simulated and experimental *S*-parameters of the manufactured prototype, whose overall circuit size is 32.5×34 mm^2 ($0.92\lambda_g \times 0.96\lambda_g$)

The measured *S*-parameters show good agreement with the simulations in Fig. 7. The measured center frequencies are almost identical to the simulated ones of 6.5 and 11 GHz. The measured 3-dB bandwidths are 540 MHz (Δ_1=8.3%) and 560 MHz (Δ_2=5.1%) compared with simulations of 545 MHz (Δ_1=8.4%) and 555 MHz (Δ_2=5.0%). In addition, the measured minimal insertion loss including that of the SMA connectors is 1.3 dB for the 1st passband, and 2.39 dB for the 2nd passband. As a comparison, the simulated ILs are 0.97 and 1.6 dB, respectively. It is noted that an extra TZ (TZ_2) is observed due

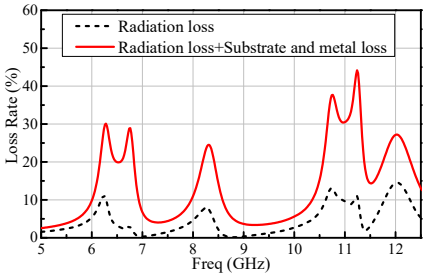

Fig. 8. Simulated loss analysis of the proposed filter under the conditions of lossy/lossless substrate and metal.

Table 1. Comparison of State-of-the-Arts Filters

Ref.	[11]	[14]	[15]		This Work
Technology	SIW & microstrip	Capacitively loaded SIW	HMSIW	HMSIW	SIW & microstrip
layer	Single	Triple	Single	Single	Single
SIW Modes	TE_{101}/TE_{201}	TE_{101}/TE_{201}	TE_{101}/TE_{301}	TE_{101}/TE_{102}	TE_{101}/TE_{301}
Order	4/4	2/2	3/3	4/4	3/3
f_1/f_2 (GHz)	8.05/9.99	2.51/5.30	5.0/7.5	5.0/8.5	6.5/11.0
$k = f_2/f_1$	1.24	2.11	1.5	1.7	1.69
3-dB FBW(%)	9.1/6.2	6.8/5.8	5.46/4.75	6.26/7.75	8.3/5.1
IL (dB)	1.74/2.21	1.41/1.88	1.65/2.25	2.02/1.82	1.3/2.39
No. of TZs	4	1	2	4	4
Size ($\lambda_g \times \lambda_g$)	1.13×1.02	0.42×0.84	1.65×0.93	0.84×1.31	0.92×0.96

to the suppression of the TE_{201} mode, leading to the improved stopband rejection between the two passbands.

Note that a dip in $|S_{11}|$ at about 8.3 GHz is observed for both the simulated and measured results. To investigate the origin of this dip, a simulated loss analysis, including radiation, substrate and metal losses, is carried out in Fig. 8. For TE_{101}, TE_{201} and TE_{301} modes, namely the modes resonating at around 6.5, 8.3 and 11 GHz, they almost suffer from the same levels of radiation loss, while the losses from the substrate and metal are much higher than radiation loss especially for the TE_{301} mode. Therefore, according to the analysis, the dip in $|S_{11}|$ at around 8.3 GHz is caused by both radiation, dielectric substrate and metal layers. The radiation loss can be taken care of in practice by inserting a patch of absorbing material above the filter.

Table 1 shows a comparison of the proposed dual-band filter with other reported filters using SIW dual-mode resonances. Compared with the filter in [11], this work presents a dual-band response with more widely separated passbands. Although a dual-band SIW filter with a large frequency ratio and a compact size is realized in [14], multilayer structures would be inevitable. While in terms of the works in [15], the proposed dual-band filter is able to create more TZs while using fewer resonators. In addition, a compact size is also achieved due to the hybrid structure of microstrip and SIW.

V. Conclusion

Two novel techniques to suppress SIW TE_{201} mode are proposed and studied. Although the TE_{201} mode is excited, its coupling path is either blocked or its contribution cancelled at the output. Compared with the conventional method of not exciting the TE_{201} mode, the proposed techniques can introduce

an extra TZ. To validate the novel concept, a dual-band SIW filter based on TE_{101} and TE_{301} modes, which shows widely separated passbands, is presented and prototyped. The design and analysis procedures are well illustrated. Compared with other reported works, the proposed filter shows an improved electrical performance with a compact filter size, which can create more TZs while using a lower-order filter configuration.

ACKNOWLEDGMENT

The authors are grateful for support by the China Scholarship Council (CSC) under Grant 202006070154, and by the Natural Sciences and Engineering Research Council (NSERC) of Canada.

REFERENCES

[1] U. Naeem, S. Bila, M. Thevenot, T. Monediere, and S. Verdeyme, "A dual-band bandpass filter with widely separated passbands," *IEEE Trans. Microw. Theory Techn.*, vol. 62, no. 3, pp. 450–456, Mar. 2014.

[2] U. Naeem, A. Périgaud, and S. Bila, "Dual-mode dual-band bandpass cavity filters with widely separated passbands," *IEEE Trans. Microw. Theory Techn.*, vol. 65, no. 8, pp. 2681–2686, Aug. 2017.

[3] S.-B. Zhang and L. Zhu, "Synthesis design of dual-band bandpass filters with $\lambda/4$ stepped-impedance resonators," *IEEE Trans. Microw. Theory Techn.*, vol. 61, no. 5, pp. 1812–1819, May 2013.

[4] M. Á. Sánchez-Soriano and R. Gómez-García, "Sharp-rejection wide-band dual-band bandpass planar filters with broadly-separated passbands," *IEEE Microw. Wireless Compon. Lett.*, vol. 25, no. 2, pp. 97-99, Feb. 2015.

[5] M. Zhou, X. Tang and F. Xiao, "Compact dual band transversal bandpass filter with multiple transmission zeros and controllable bandwidths," *IEEE Microw. Wireless Compon. Lett.*, vol. 19, no. 6, pp. 347-349, June 2009.

[6] W. Jiang, W. Shen, T. Wang, Y. M. Huang, Y. Peng and G. Wang, "Compact dual-band filter using open/short stub loaded stepped impedance resonators (OSLSIRs/SSLSIRs)," *IEEE Microw. Wireless Compon. Lett.*, vol. 26, no. 9, pp. 672-674, Sept. 2016.

[7] B. Ren et al., "Miniature dual-band bandpass filter using modified quarter-wavelength SIRs with controllable passbands," *Electron. Lett.*, vol. 55, no. 1, pp. 38–40, Jan. 2019.

[8] S. Lee and Y. Lee, "A planar dual-band filter based on reduced-length parallel coupled lines," *IEEE Microw. Wireless Compon. Lett.*, vol. 20, no. 1, pp. 16-18, Jan. 2010.

[9] F. Bagci, A. Fernández-Prieto, A. Lujambio, J. Martel, J. Bernal and F. Medina, "Compact balanced dual-band bandpass filter based on modified coupled-embedded resonators," *IEEE Microw. Wireless Compon. Lett.*, vol. 27, no. 1, pp. 31-33, Jan. 2017.

[10] K. Zhou, C. Zhou, and W. Wu, "Resonance characteristics of substrate-integrated rectangular cavity and their applications to dual-band and wide-stopband bandpass filters design," *IEEE Trans. Microw. Theory Techn.*, vol. 65, no. 5, pp. 1511-1524, May 2017.

[11] Y. Zhu and Y. Dong, "A compact dual-band quasi-elliptic filter based on hybrid SIW and microstrip technologies," *IEEE Trans. Circuits Syst. II, Exp. Briefs*, in press, doi: 10.1109/TCSII.2021.3111860.

[12] A. R. Azad and A. Mohan, "Substrate integrated waveguide dual-band bandpass filter," in *Proc. IEEE 8th Uttar Pradesh Sect. Int. Conf. Electr. Electron. Comput. Eng. (UPCON)*, Dehradun, India, Nov. 2021, pp. 1–6.

[13] A. R. Azad and A. Mohan, "Substrate integrated waveguide dual-band and wide-stopband bandpass filters," *IEEE Microw. Wireless Compon. Lett.*, vol. 28, no. 8, pp. 660-662, Aug. 2018.

[14] M. Li, C. Chen and W. Chen, "Miniaturized dual-band filter using dual-capacitively loaded SIW cavities," *IEEE Microw. Wireless Compon. Lett.*, vol. 27, no. 4, pp. 344-346, April 2017.

[15] K. Zhou, C. Zhou, and W. Wu, "Dual-mode characteristics of half-mode SIW rectangular cavity and applications to dual-band filters with widely separated passbands," *IEEE Trans. Microw. Theory Techn.*, vol. 66, no. 11, pp. 4820-4829, Nov. 2018.

[16] J. S. Hong and M. J. Lancaster, *Microstrip Filters for RF/Microwave Applications*. New York, NY, USA: Wiley, 2001, chs. 8–10.